Multilead Analysis of T-Wave Alternans in the ECG Using Principal Component Analysis

Violeta Monasterio*, Pablo Laguna, *Senior Member, IEEE*, and Juan Pablo Martínez

***Abstract*—T-wave alternans (TWA) is a cardiac phenomenon associated with the mechanisms leading to sudden cardiac death. Several methods exist to automatically detect and estimate TWA in the ECG on a single-lead basis, and their main drawback is their poor sensitivity to low-amplitude TWA. In this paper, we propose a multilead analysis scheme to improve the detection and estimation of TWA. It combines principal component analysis with a single-lead method based on the generalized likelihood ratio test. The proposed scheme is evaluated and compared to a single-lead scheme by means of a simulation study, in which different types of simulated and physiological noise are considered under realistic conditions. Simulation results show that the multilead scheme can detect TWA with an SNR 30 dB lower and allows the estimation of TWA with an SNR 25 dB lower than the single-lead scheme. The two analysis schemes are also applied to stress test ECG records. Results show that the multilead scheme provides a higher detection power and that TWA detections obtained with this scheme are significantly different in healthy volunteers and ischemic patients, whereas they are not with the single-lead scheme.**

***Index Terms*—ECG, multilead analysis, principal component analysis (PCA), T-wave alternans (TWA).**

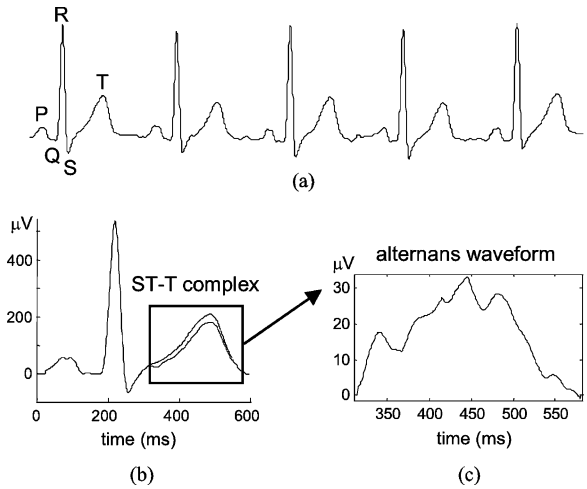

Fig. 1. (a) ECG signal with visible TWA. (b) Superposition of two consecutive beats. (c) Alternans waveform: difference between odd and even beats.

I. Introduction

T-WAVE alternans (TWA) is a cardiac phenomenon extensively studied as an index of high risk of malignant arrhythmias and sudden cardiac death (SCD) [1], [2]. This paper presents a multilead analysis scheme that improves the detection and estimation of TWA in the ECG.

ECG signals are measured by placing electrodes on the body surface and recording the electrical activity of the heart. The simultaneous recording of the ECG on different chest locations (channels or leads) provides a spatial perception of cardiac events. The standard 12-lead system is the most widely used system in clinical practice, and consists of eight independent leads, named V1–V6, I, and II, and four additional leads that can be derived from the independent ones. The ECG usually presents three characteristic waves on each beat: P-wave, QRS complex, and T-wave [Fig. 1(a)]. The interval between the end of the QRS complex and the end of the T-wave is known as ST-T complex, and reflects the repolarization activity of the ventricles.

TWA is defined as a consistent fluctuation in the repolarization morphology on an every-other-beat basis [Fig. 1(b) and (c)]. TWA amplitude is in the range of microvolts and can be even below the noise level, making its detection a difficult task. Several signal processing methods exist to detect and estimate TWA. A comprehensive review can be found in [3]. The most widely used techniques are the spectral method (SM) [1], [4] and the modified moving average method [5]. Alternative techniques are the complex demodulation method [6] and the recently proposed Laplacian likelihood ratio method (LLR) [7], [8]. The main drawback of existing techniques is either their sensitivity to the presence of nonalternant components with high amplitude or their poor sensitivity to low-level TWA [2], [3]. Furthermore, some of these techniques measure TWA amplitude, but do not estimate the TWA waveform. An accurate waveform estimation is desirable because, in addition to the presence and magnitude of TWA, the distribution of TWA within the ST-T complex has been shown to indicate arrhythmic risk [9].

To date, TWA analysis techniques have been mostly applied to each lead individually. In commercial TWA analysis systems, only basic multilead strategies are performed, such as analyzing the vector-magnitude lead (CH2000 and Heartwave systems, Cambridge Heart, Inc., Bedford, MA). However, ECG signals present a high spatial redundancy that can be better exploited with techniques based on the eigenanalysis of input data, such as

Manuscript received October 3, 2008; revised January 15, 2009. First published March 4, 2009; current version published June 12, 2009. This work was supported by the Centro de Investigación Biomédica en Red (CIBER) de Bioingeniería, Biomateriales y Nanomedicina through Instituto de Salud Carlos III (ISCIII), by the Comisión Interministerial de Ciencia y Tecnología (CICYT) under Project TEC-2007-68076-C02-02, and by the Grupo Consolidado T30 (Spain). *Asterisk indicates corresponding author*.

*V. Monasterio is with the Centro de Investigación Biomédica en Red de Bioingeniería, Biomateriales y Nanomedicina (CIBER-BBN), Communications Technology Group, Aragón Institute of Engineering Research, University of Zaragoza, Zaragoza 50018, Spain (e-mail: violeta.monasterio@unizar.es).

P. Laguna and J. P. Martínez are with the Centro de Investigación Biomédica en Red de Bioingeniería, Biomateriales y Nanomedicina (CIBER-BBN), Communications Technology Group, Aragón Institute of Engineering Research, University of Zaragoza, Zaragoza 50018, Spain (e-mail: laguna@unizar.es; jpmart@unizar.es).

Digital Object Identifier 10.1109/TBME.2009.2015935

principal component analysis (PCA) or Karhunen–Loève transform (KLT) [10]. These techniques have been applied to ECG data compression and noise reduction [11]–[14], characterization and diagnosis of ischemia [15], [16], repolarization heterogeneity [17]–[19], atrial fibrillation [20], [21], and separation of maternal and fetal ECG [22]. The hypothesis of this paper is that TWA analysis can be improved by exploiting the spatial redundancy of ECG signals with PCA.

In this paper, we propose a multilead TWA analysis scheme that combines PCA with the LLR method [7], [8]. As stated in [3], methodological evaluation of a new technique (i.e., the quantification of its detection power and its estimation accuracy) is a prior step to clinical validation (which quantifies the adequateness of the TWA test as a risk stratifier). In this paper, we present a complete methodological evaluation of the proposed scheme by means of a simulation study, where the proposed scheme is compared to a single-lead scheme, which is the usual approach to TWA analysis. We also provide an example of application to real signals, to show that the performance improvement observed in simulation can also be obtained in real datasets.

II. Methods for TWA Analysis

A. LLR Method

The LLR method computes beat-to-beat the maximum likelihood estimation (MLE) of the TWA under the assumption of Laplacian noise, and applies a generalized likelihood ratio test (GLRT) to decide whether TWA is present or not.

Let K be the number of beats under analysis, N the number of samples of each ST-T complex, and L the number of leads. The ST-T complex of the kth beat and the lth lead is denoted as

$$\mathbf{x}_{k,l} = [\, x_{k,l}(0) \quad \cdots \quad x_{k,l}(N-1) \,]^T . \tag{1}$$

The LLR method assumes the following model for each complex:

$$x_{k,l}(n) = s_l(n) + \frac{1}{2} a_l(n)(-1)^k + v_{k,l}(n), \quad n = 0, \ldots, N-1 \tag{2}$$

which, in vector notation, is

$$\mathbf{x}_{k,l} = \mathbf{s}_l + \frac{1}{2}\boldsymbol{a}_l(-1)^k + \mathbf{v}_{k,l} \tag{3}$$

where $\boldsymbol{s}_l$ is the background ST-T complex, which is periodically repeated in every beat, $\boldsymbol{a}_l$ is the TWA waveform (defined as the difference between odd and even beats), and $\boldsymbol{v}_{k,l}$ is the additive random noise [vectors in (3) are defined as in (1)].

Background ST-T complexes can be canceled with a detrending filter that computes the difference between each complex and the previous one

$$\mathbf{x}'_{k,l} = \mathbf{x}_{k,l} - \mathbf{x}_{k-1,l}, \qquad k = 1, \ldots, K-1. \tag{4}$$

The noise present in $\mathbf{x}'_{k,l}$ is assumed to be independent and identically distributed Laplacian with zero mean and unknown standard deviation σ_l. The MLE of $\boldsymbol{a}_l$ for this model is given by [7], [8]

$$\hat{a}_l(n) = \text{median}\left(\left\{ x'_{k,l}(n)(-1)^k \right\}_{k=1}^{K-1} \right), \quad n = 0, \ldots, N-1. \tag{5}$$

TWA amplitude is calculated as the rms value across the TWA waveform

$$V_l = \sqrt{\frac{1}{N}\sum_{n=0}^{N-1} \hat{a}_l^2(n)} \quad \text{(in microvolts)}. \tag{6}$$

The GLRT statistic can be expressed as

$$Z_l = \frac{\sqrt{2}}{\hat{\sigma}_l} \sum_{n=0}^{N-1} \left(\sum_{k=1}^{K-1} \left| x'_{k,l}(n) \right| - \sum_{k=1}^{K-1} \left| x'_{k,l}(n) - \hat{a}_l(n)(-1)^k \right| \right) \tag{7}$$

where $\hat{\sigma}_l$ is the MLE of the standard deviation of the noise

$$\hat{\sigma}_l = \frac{\sqrt{2}}{2NK} \sum_{k=1}^{K-1} \left\| \mathbf{x}'_{k,l} - \hat{\boldsymbol{a}}_l(-1)^k \right\|_1 . \tag{8}$$

Details of the derivation of the MLE and GLRT can be found in [7] and [8] and are beyond the scope of this paper. To decide whether TWA is present or not, the GLRT statistic Z_l is compared to a threshold γ. TWA detection is positive if $Z_l > \gamma$ and negative otherwise. Since the detection statistic (7) is invariant to amplitude scaling of $\mathbf{x}'_{k,l}$ (i.e., it is a constant false alarm rate (CFAR) detector), the value of γ can be set to obtain a fixed probability of false alarm (P_{FA}) regardless of the noise level.

B. Spectral Method

The SM [1], [4] is based on Fourier analysis of each beat-to-beat series of synchronized samples within the ST-T complex. The TWA component is obtained by evaluating the short-time Fourier transform (STFT) at the alternans frequency, i.e., 0.5 cycles per beat (cpb). According to [3], the detection statistic can be expressed as $Z_l = (1/N)\sum_{n=0}^{N-1} z_l(n)$, where $z_l(n) = (1/K)\left|\text{STFT}\left\{x_{k,l}(n)\right\}\right|^2_{f=0.5}$ is the 0.5 cpb bin of the short-time periodogram computed from the beat-to-beat series of the nth sample. A significance measure called TWA ratio (TWAR) is defined as

$$\text{TWAR}(l) = \frac{Z_l - m_l}{s_l} \tag{9}$$

where m_l and s_l are the mean and the standard deviation of the spectral noise measured in the spectral window [0.33–0.48 cpb]. To evaluate whether TWA is significant, TWAR is compared to a fixed threshold (typically $\gamma = 3$). Finally, TWA amplitude is estimated as

$$V_l = \sqrt{Z_l - m_l} \quad \text{(in microvolts)}. \tag{10}$$

C. Multilead Scheme

The block diagram of the proposed multilead scheme is shown in Fig. 2(a). It consists of five stages: signal preprocessing, signal transformation with PCA, TWA detection, signal reconstruction, and TWA estimation.

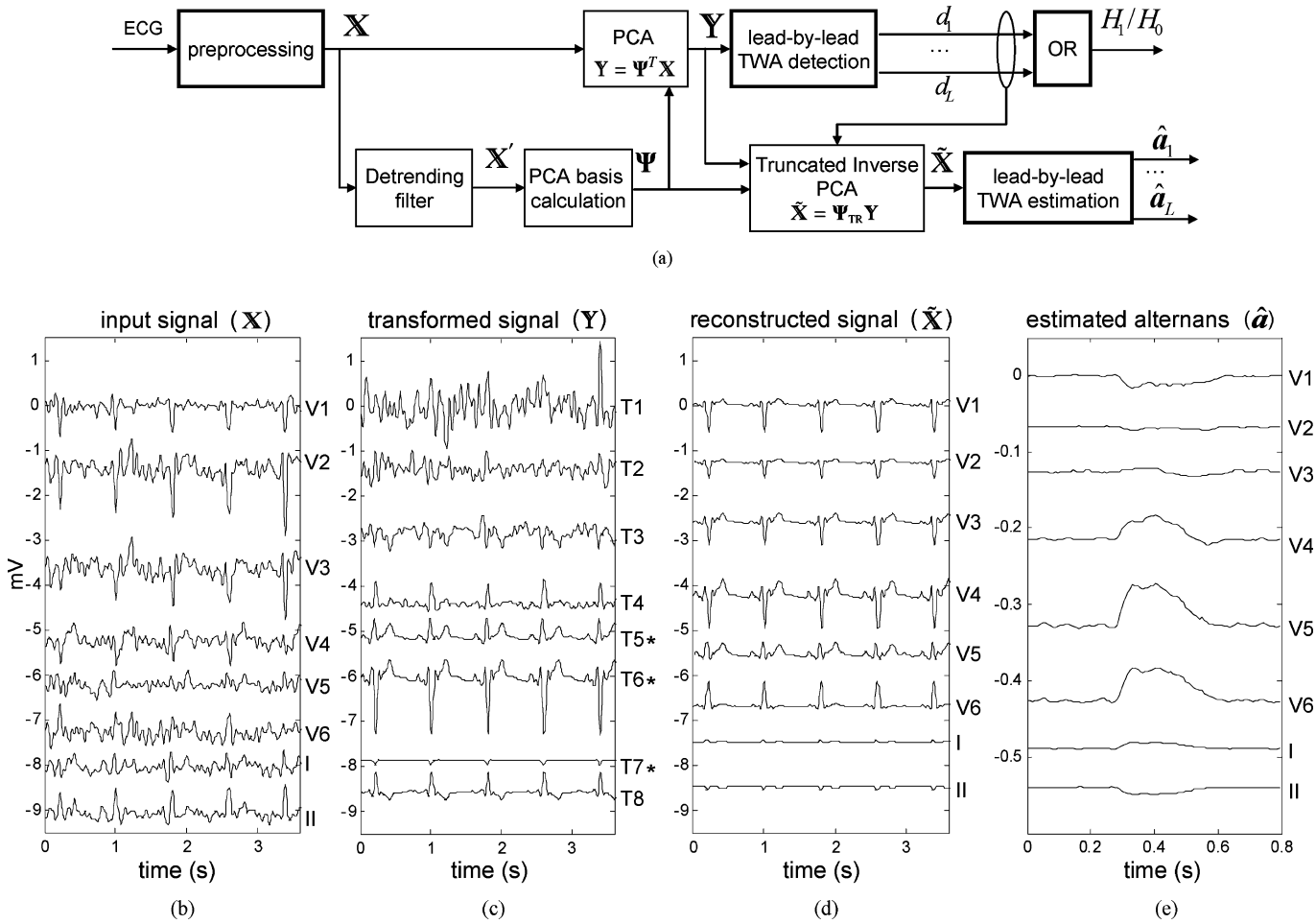

Fig. 2. (a) Block diagram of the multilead scheme. The blocks in bold line are the ones used in the single-lead scheme. Note that in the single-lead scheme, $\mathbb{Y} = \mathbb{X} = \tilde{\mathbb{X}}$. (b) Simulated input signal with SNR $= -20$ dB. (c) Transformed signal after PCA. Asterisks indicate the leads where TWA is detected ($d_5 = d_6 = d_7 = 1$). (d) Reconstructed signal after truncated inverse PCA. (e) Estimated TWA waveform. Note that TWA is visible in T5 and V5 in the reconstructed signal.

1) Signal Preprocessing: The ECG signal is preprocessed as follows. QRS positions are determined using a wavelet-based algorithm [23]. Baseline wander is removed with a cubic splines interpolation technique. The signal is then decimated to obtain a sampling frequency of $F_s = 125$ Hz and low-pass-filtered with a cutoff frequency of 15 Hz. Fig. 2(b) shows a simulated example of multilead ECG signal after the preprocessing stage.

A fixed interval of 350 ms after each QRS fiducial point is selected for TWA analysis (ST-T complexes). For each beat k, complexes from all leads are put together into a matrix $\mathbf{X}_k$

$$\mathbf{X}_k = [\,\mathbf{x}_{k,1} \quad \cdots \quad \mathbf{x}_{k,L}\,]^T. \tag{11}$$

The nth column of $\mathbf{X}_k$ contains the amplitudes of the L leads at a given sample n of the kth beat. The $\mathbf{X}_k$ matrices are then concatenated to form the data matrix $\mathbb{X}$

$$\mathbb{X} = [\,\mathbf{X}_0 \quad \mathbf{X}_1 \quad \cdots \quad \mathbf{X}_{K-1}\,]. \tag{12}$$

The lth row of $\mathbb{X}$ contains the concatenated ST-T complexes corresponding to the lth lead.

2) Signal Transformation With PCA: After the preprocessing stage, a detrending filter is applied to $\mathbb{X}$ to cancel the background ST-T complexes as in (4). The resulting matrix $\mathbb{X}'$ has the same structure as $\mathbb{X}$ (this time with $K-1$ beats), i.e., the lth row contains the concatenation of the detrended complexes corresponding to the lth lead. PCA basis is then calculated from matrix $\mathbb{X}'$. The detrended signal $\mathbb{X}'$ is a zero-mean random process with a spatial correlation matrix $\mathbf{R}_{\mathbb{X}'} = E\{\mathbb{X}'\mathbb{X}'^T\}$. In practice, $\mathbf{R}_{\mathbb{X}'}$ is replaced by the sample correlation matrix, defined as

$$\hat{\mathbf{R}}_{\mathbb{X}'} = \frac{1}{(K-1)N}\mathbb{X}'\mathbb{X}'^T. \tag{13}$$

To obtain the set of L principal components of $\mathbb{X}'$, the eigenvector equation for $\hat{\mathbf{R}}_{\mathbb{X}'}$ must be solved

$$\hat{\mathbf{R}}_{\mathbb{X}'}\mathbf{\Psi} = \mathbf{\Psi}\mathbf{\Lambda} \tag{14}$$

where $\mathbf{\Lambda}$ denotes the diagonal eigenvalue matrix and $\mathbf{\Psi}$ denotes the eigenvector matrix. Matrix $\mathbf{\Psi}$ defines an orthonormal transformation, which is applied to the original data $\mathbb{X}$

$$\mathbb{Y} = \mathbf{\Psi}^T\mathbb{X}. \tag{15}$$

The lth row of $\mathbb{Y}$ contains the lth principal component of $\mathbb{X}$, and we will refer to it as the lth transformed lead (Tl) from here on. Fig. 2(c) shows the transformed signal for the example case.

3) TWA Detection: After PCA transformation, TWA detection is performed in the transformed data. The GLRT is applied to each transformed lead (rows in $\mathbb{Y}$), as shown in Section II-A. The result of this lead-by-lead detection is denoted as d_l: $d_l = 1$ if TWA is detected in the lth transformed lead and $d_l = 0$ otherwise. The overall TWA detection is positive if TWA is detected at least in one transformed lead ["OR" block in Fig. 2(a)].

4) Signal Reconstruction With Inverse PCA: After TWA detection, a new signal in the original lead set is reconstructed. This is necessary because TWA must be measured in the original leads to be useful in clinical practice. A diagonal matrix is defined from the lead-by-lead detection as

$$\mathbb{A} = \begin{bmatrix} d_1 & & 0 \\ & \ddots & \\ 0 & & d_L \end{bmatrix} \tag{16}$$

and the basis in $\mathbf{\Psi}$ is truncated as follows:

$$\mathbf{\Psi}_{\mathrm{TR}} = \mathbf{\Psi}\mathbb{A}. \tag{17}$$

Matrix $\mathbf{\Psi}_{\mathrm{TR}}$ has zeros in columns corresponding to leads without TWA. A reconstructed signal is then obtained from the leads with detected TWA as

$$\tilde{\mathbb{X}} = \mathbf{\Psi}_{\mathrm{TR}}\mathbb{Y}. \tag{18}$$

The reconstructed data matrix $\tilde{\mathbb{X}}$ consists of the concatenation of the multilead single-beat matrices $\tilde{\mathbf{X}}_k$

$$\tilde{\mathbb{X}} = [\,\tilde{\mathbf{X}}_0 \quad \tilde{\mathbf{X}}_1 \quad \cdots \quad \tilde{\mathbf{X}}_{K-1}\,] \tag{19}$$

where

$$\tilde{\mathbf{X}}_k = [\,\tilde{\mathbf{x}}_{k,1} \quad \cdots \quad \tilde{\mathbf{x}}_{k,L}\,]^T \tag{20}$$

with $\tilde{\mathbf{x}}_{k,l}$ corresponding to the reconstructed ST-T complex of the kth beat in the lth lead. Note that $\tilde{\mathbb{X}} = \left(\mathbf{\Psi}\mathbb{A}\mathbf{\Psi}^T\right)\mathbb{X}$ is equivalent to a spatially filtered version of $\mathbb{X}$, where the aim of the equivalent filter is to preserve the TWA content, not to obtain a perfect signal reconstruction. When no detection is obtained, $\tilde{\mathbb{X}} = 0$. Fig. 2(d) shows the reconstructed signal for the example case.

5) TWA Estimation: To estimate the TWA waveform and amplitude, the MLE is applied to the reconstructed data, as described in Section II-A. Fig. 2(e) shows the estimated TWA for the example case.

D. Single-Lead Scheme

The single-lead scheme handles each lead independently throughout the process. It consists of the same signal preprocessing, TWA estimation, and TWA detection stages as the multilead scheme, but without the intermediate PCA processing. Detection and estimation are performed directly in the original leads, i.e., $\mathbb{Y} = \mathbb{X} = \tilde{\mathbb{X}}$. The stages of the single-lead scheme are shown in bold in Fig. 2(a).

Both the multilead and the single-lead scheme can be easily adapted to TWA analysis methods other than the LLR method. For example, they can be combined with the SM method by substituting the GLRT-based decision rule (Section II-A) by a TWAR-based decision rule (Section II-B) and by substituting the amplitude estimation in (6) by the estimation in (10).

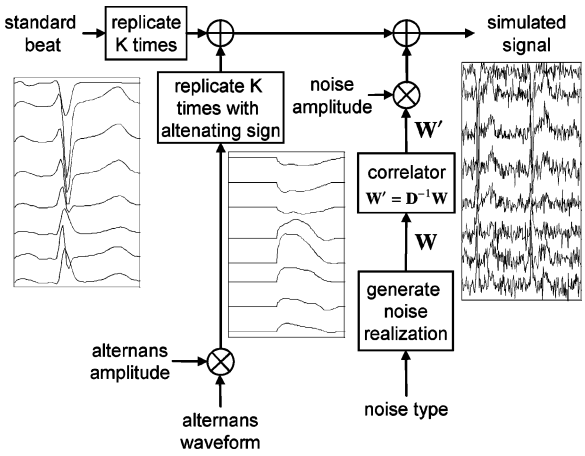

Fig. 3. Simulation of multilead ECG signals with TWA and noise. Signals scale is not preserved for better visualization.

III. Datasets

A. Simulated Data

Biomedical signal processing techniques are usually evaluated on standard databases, where the output of the technique is compared to reference annotations established by experts. However, the main problem in the case of TWA analysis is the lack of validation databases, mainly because TWA is often nonvisible due to its low amplitude (sometimes below the noise level). Therefore, in this paper, a Monte Carlo simulation approach was adopted. To evaluate the multilead scheme and compare it with the single-lead scheme, we designed a simulation study where synthetic ECG signals were created with a high degree of realism and where TWA parameters (amplitude, waveform) were known *a priori*.

Multilead ECG signals were generated adding noise and TWA to a clean background ECG. Fig. 3 shows the simulation setup. A standard beat from a 12-lead ECG record was selected to create the background ECG. A TWA waveform was detected and extracted from another 12-lead record, using the LLR method as described in [8]. Both records belonged to the STAFF-III database [8]. From the 12-lead set, we only selected the independent leads ($L = 8$).

Four types of noise were considered: Gaussian (gs), Laplacian (lp), electrode motion (em), and muscular activity (ma). Noise types gs and lp were randomly generated. Types em and ma, which are typical noises present in the ECG, were extracted from two real noise records of the MIT-BIH Noise Stress Test Database [24]. These records were obtained using a Holter recorder on an active subject with leads placed so that the subject's ECG was not visible. Record em contains electrode motion artifact (usually the result of intermittent mechanical forces acting on the electrodes), with significant amounts of baseline wander and muscle noise as well. Record ma contains primarily muscle noise, with a spectrum that overlaps that of the ECG, but that extends to higher frequencies.

Each Monte Carlo trial was generated as the sum of the background ECG beat repeated K times, the TWA waveform repeated K times with alternating sign, and a random realization of noise. Each realization of noise was generated as follows. First, L segments of $K \times N$ samples were simulated (gs or lp noise) or extracted from the records beginning at a random position (em or ma noise). Baseline wander was removed from em and ma noises, because em and ma records contain low-frequency variations of high amplitude that can distort the level of noise added to the simulated ECG. Noise segments were normalized to a 1 μV rms value and piled to form a multilead matrix $\mathbf{W}$

$$\mathbf{W} = [\, \mathbf{w}_1 \quad \cdots \quad \mathbf{w}_L \,]^T . \tag{21}$$

Due to the noise generation setup, noise segments $\mathbf{w}_l$ are spatially uncorrelated ($\mathbf{R}_W = \mathbb{I}$). However, in real signals, noise is spatially correlated. To correlate $\mathbf{W}$ in a realistic way, we first estimated the spatial correlation of real ECG noise using ten multilead ECG records of the PTB Diagnostic ECG Database [25]. We selected 2000 segments of noise from each independent lead by taking the 50 ms interval prior to a P-wave onset for each segment. DC level was removed and segments corresponding to each lead were concatenated. The resulting noise leads were piled as in (21) to form a noise matrix $\mathbf{N}$. The spatial correlation of $\mathbf{N}$ was estimated as

$$\hat{\mathbf{R}}_N = \frac{1}{M}\mathbf{N}\mathbf{N}^T \tag{22}$$

where M is the number of samples of each noise lead. Applying the Cholesky decomposition [26] to the inverse of the correlation matrix, we obtained

$$\hat{\mathbf{R}}_N^{-1} = \mathbf{D}^T\mathbf{D} \tag{23}$$

where $\mathbf{D}$ is an upper triangular matrix with strictly positive diagonal entries. The inverse of $\mathbf{D}$ was used to spatially correlate the generated noise $\mathbf{W}$

$$\mathbf{W}' = \mathbf{D}^{-1}\mathbf{W} \tag{24}$$

thus obtaining a correlated noise matrix $\mathbf{W}'$ with a spatial correlation $\mathbf{R}_{\mathbf{W}'} = \hat{\mathbf{R}}_N$. Finally, the correlated noise $\mathbf{W}'$ was scaled so that the rms value of the least noisy lead was 200 μV. TWA was then scaled to obtain a desired SNR level, defined as the maximum ratio between TWA power and noise power in the L leads.

We simulated multilead ECG signals with SNR levels ranging from -60 to 10 dB and also without TWA. For each type of noise, we generated 10^4 realizations of noise to simulate signals without TWA and 10^4 realizations for each SNR level to generate signals with TWA.

B. Stress Test Data

As an example of application to real data, TWA analysis was performed on set of stress test ECG records. The ECGs of 136 patients referred to treadmill exercise test (following Bruce Protocol) were recorded in the University Hospital Lozano Blesa of Zaragoza (Spain) [27]. Standard leads (V1, V3–V6, I, II, III, aVR, aVL, and aVF) and RV4 were digitally recorded at 1-kHz sampling rate with an amplitude resolution of 0.6 μV. Patients were classified in two groups.

1) Ischemic group: This group was composed of 79 patients with significant stenoses in at least one major coronary artery as shown by coronary angiography (gold standard).

2) Volunteer group: This group comprised 66 asymptomatic volunteers from the Spanish Army, who underwent an exercise test with negative results for coronary artery disease.

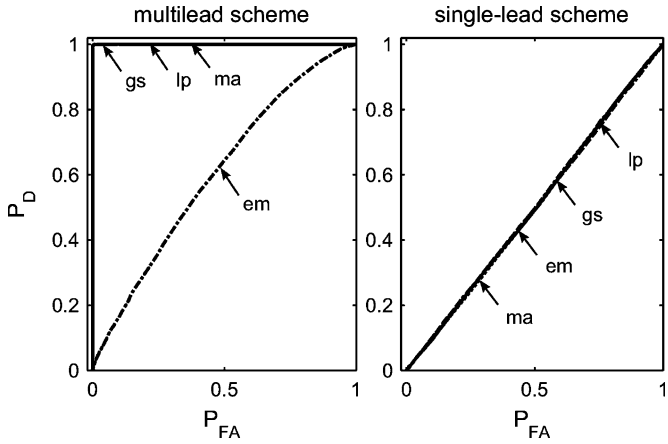

Fig. 4. ROC curves for SNR $= -45$ dB of (left) the multilead scheme and (right) the single-lead scheme combined with LLR method.

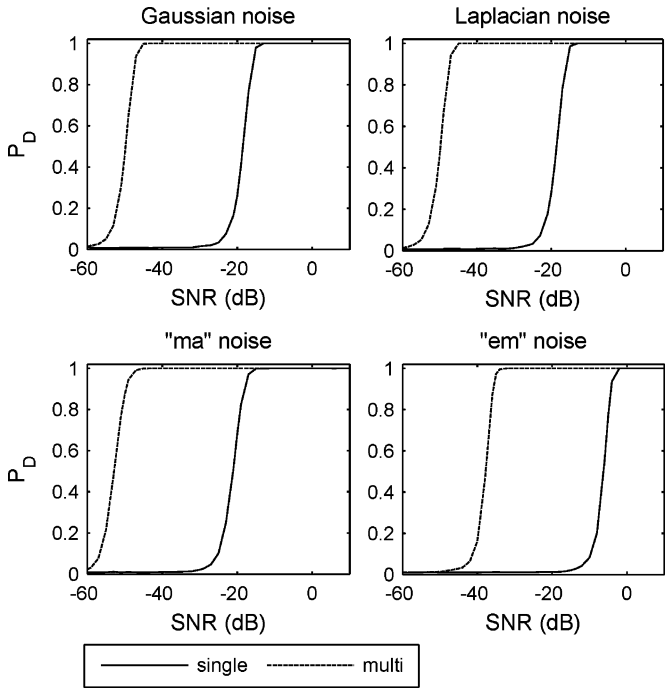

Fig. 5. P_{D} for $P_{\mathrm{FA}} = 0.01$ of the single-lead (solid line) and the multilead scheme (dashed line) combined with LLR method versus SNR. Results obtained with an analysis window of 32 beats.

IV. Results

A. Simulated Data

Simulated signals were processed with the two schemes based on the LLR method using a 32-beat analysis window; for both

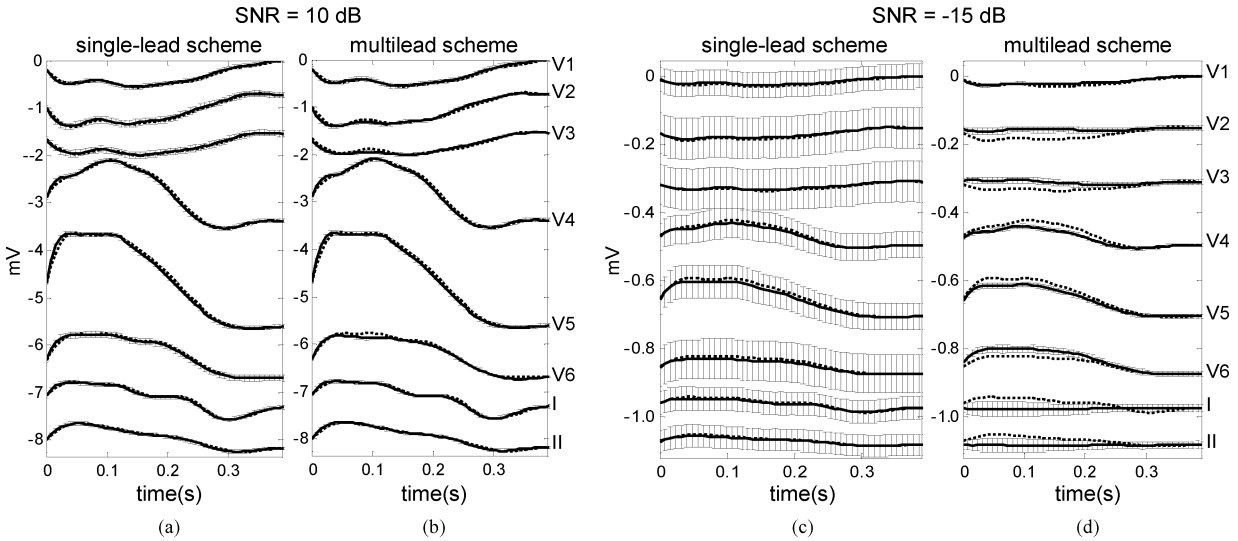

Fig. 6. Expected value $E\{\hat{a}_l(n)\}$ (solid line) and standard deviation $\sigma_{\hat{a}_l}(n)$ (vertical bars) of the TWA waveforms estimated with the LLR method, obtained with (a) the single-lead and (b) the multilead scheme for SNR $= 10$ dB, and with (c) the single-lead and (d) the multilead scheme for SNR $= -15$ dB for gs noise. True TWA shown in dashed line. Leads offset included for better visualization.

schemes, we studied the detection performance and the accuracy of the estimation. Furthermore, simulated signals with ma noise were processed combining the two analysis schemes with LLR and SM methods, with a 128-beat analysis window.

1) Detection Performance: Detection performance was evaluated with receiver operating characteristic (ROC) curves, which show the relationship between probability of detection ($P_{\rm D}$) and probability of false alarm ($P_{\rm FA}$) as a function of the detection threshold γ. For every type of noise and SNR level, the area under the ROC curve of the multilead scheme was greater than the area under the single-lead curve. Fig. 4 shows the ROC curves corresponding to SNR $= -45$ dB.

To analyze the behavior of the schemes for different SNR levels, we selected a fixed value for γ so that $P_{\rm FA} = 0.01$, and compared the resulting $P_{\rm D}$. Fig. 5 shows $P_{\rm D}$ of the two schemes versus SNR for all types of noise. The SNR level where $P_{\rm D}$ starts decreasing is 30 dB lower with the multilead scheme than with the single-lead scheme for gs and lp noises, 28 dB lower for em noise, and 27 dB lower for ma noise.

2) Estimation Accuracy: The estimation performance of the two schemes was evaluated in terms of bias, variance, and mean square error. Let us denote by $\hat{a}_l(n)$ the nth sample of the estimated TWA waveform in the lth lead and by $a_l(n)$ the same sample of the true TWA waveform. For each SNR level, the expected value of the estimation $E\{\hat{a}_l(n)\}$ and the standard deviation $\sigma_{\hat{a}_l}(n)$ were estimated as the average and the standard deviation of $\hat{a}_l(n)$ in the 10^4 realizations, respectively. Fig. 6 shows the expected value and the standard deviation of the estimation for gs noise and two SNR levels. The bias of the multilead estimation is higher than the bias of the single-lead estimation in both cases, but the standard deviation of the multilead estimation is lower. For each SNR level and lead l, bias and mean square error of the estimation were calculated as

$$b_l(n) = E\{\hat{a}_l(n)\} - a_l(n), \qquad n = 0, \ldots, N-1 \tag{25}$$

$$e_l^2(n) = E\{(\hat{a}_l(n) - a_l(n))^2\}, \quad n = 0, \ldots, N-1 \tag{26}$$

where the expected values were estimated as the average of the 10^4 realizations. Then, two performance parameters, $\mathcal{R}_{b_l}$ and $\mathcal{R}_{e_l}$, were defined as

$$\mathcal{R}_{b_l}(\%) = \frac{\sqrt{(1/N)\sum_{n=0}^{N-1} b_l^2(n)}}{\sqrt{(1/N)\sum_{n=0}^{N-1} a_l^2(n)}} \times 100 \tag{27}$$

$$\mathcal{R}_{e_l}(\%) = \frac{\sqrt{(1/N)\sum_{n=0}^{N-1} e_l^2(n)}}{\sqrt{(1/N)\sum_{n=0}^{N-1} a_l^2(n)}} \times 100. \tag{28}$$

Parameter $\mathcal{R}_{b_l}$ measures the relative bias of the estimation in the lth lead, and parameter $\mathcal{R}_{e_l}$ measures the relative error caused by both the bias and the variance of the estimation. Fig. 7 shows the evolution of $\mathcal{R}_{b_l}$ and $\mathcal{R}_{e_l}$ versus SNR for ma noise. For SNR ≥ -15 dB, the bias of the multilead estimation is higher than the bias of the single-lead estimation. For SNR < -15 dB, the bias of the single-lead estimation tends to 100% for all the leads. For high SNR levels, $\mathcal{R}_{e_l}$ is similar for both schemes, and for low SNR levels, it is lower for the multilead scheme.

3) Comparison With SM: Simulated signals with ma noise were processed with the two schemes combined with LLR method (*LLR single* and *LLR multi*) and also with the two schemes combined with SM method (*SM single* and *SM multi*). A 128-beat analysis window was used in all cases. To ensure an unbiased comparison, detection thresholds were set so that the resulting $P_{\rm FA}$ was 0.01 for every technique. Detection curves for all techniques are shown in Fig. 8. Best results are obtained with the *LLR multi* technique. The SNR level where $P_{\rm D}$ starts decreasing is 8 dB lower for *LLR single* than for *SM single*, 6 dB lower for *LLR multi* than for *SM multi*, 30 dB lower for *SM multi* than for *SM single*, and 28 dB lower for *LLR multi* than for *LLR single*.

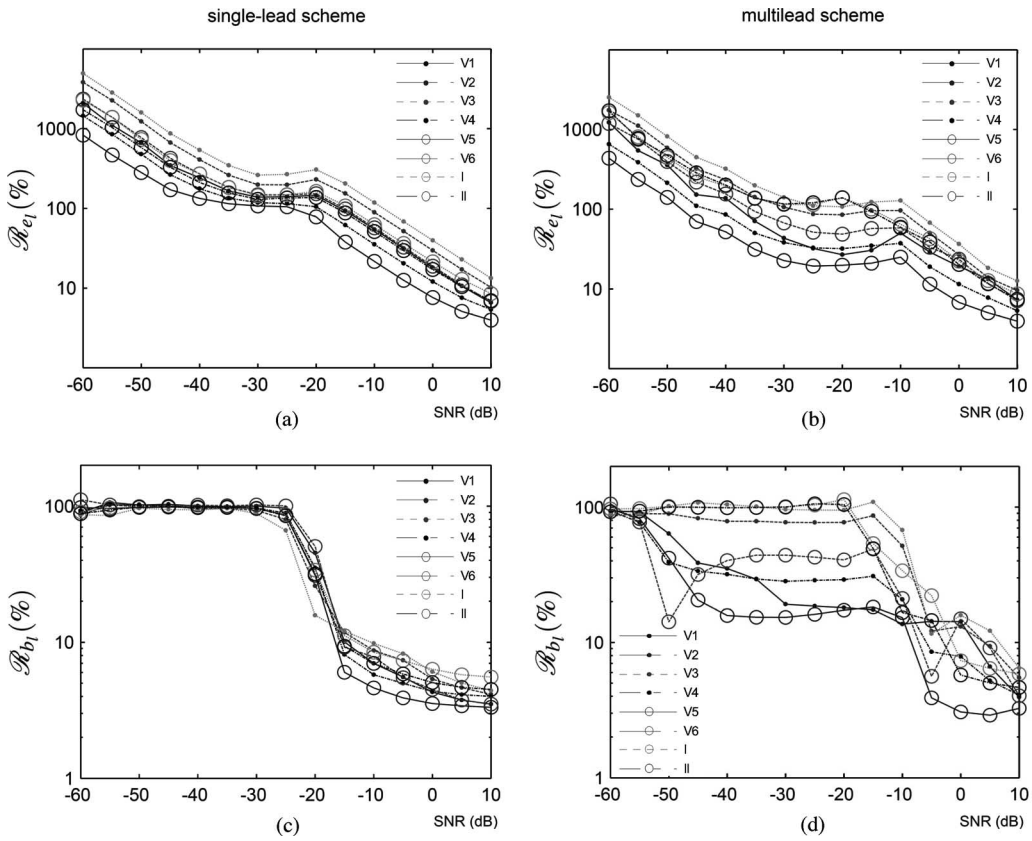

Fig. 7. Relative error of the TWA estimation obtained with the LLR method combined with (a) the single-lead and (b) the multilead scheme versus SNR, and relative bias of the estimation with the (c) single-lead and (d) the multilead scheme versus SNR for ma noise.

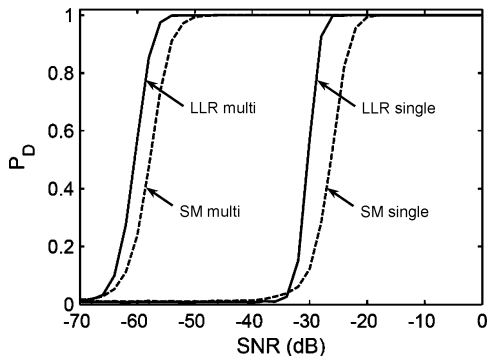

Fig. 8. $P_{\rm D}$ versus SNR for single-lead scheme combined with the LLR method (LLR single) and with the spectral method (SM single), and for multilead scheme combined with the LLR method (LLR multi) and with the SM method (SM multi). $P_{\rm FA} = 0.01$ in all cases. Results obtained with an analysis window of 128 beats.

B. Stress Test Data

Stress test records were processed using a sliding analysis window of 128 beats with the two schemes combined with the LLR method. Only the eight independent leads were considered. TWA is a phenomenon partially related to heart rate, so TWA arises in patients at risk for SCD but also in healthy subjects at faster heart rates during stress tests. Therefore, the assumption that no TWA should be found in volunteer records at heart rates below a cutoff heart rate HR_c was made to set the same $P_{\rm FA} = 0.01$ for both analysis schemes. Volunteer's signals were processed, and for each scheme, a threshold was calculated so that it was exceeded only by 1% of the Z-values obtained before heart rate reached HR_c (false detections). Then, all records from both groups were processed with the resulting thresholds. Table I shows results obtained considering $\mathrm{HR}_c = 110$ beats per minute (bpm) to set the $P_{\rm FA}$. The first row shows the total number of records of each group and the number of records where one or more TWA episodes were detected. For each episode, three parameters were calculated: the maximum TWA amplitude in the episode $V_{\max}$ (in microvolt), the duration $\mathcal{D}$ (in seconds), and the onset heart rate HR_o (in beats per minute), which was calculated as the mean heart rate of the analysis window in which the episode begins. For each group, the mean value and the standard deviation of these parameters were calculated in two ways: considering all the episodes (second row) and considering the episodes detected exclusively by one scheme and not by the other (third row). Table II shows the number of records where TWA episodes were detected before 110 bpm ($P_{\rm FA}$ set with an $\mathrm{HR}_c = 110$ bpm) and the number of records where TWA episodes were detected before 100 bpm ($P_{\rm FA} = 0.01$ set with an $\mathrm{HR}_c = 100$ bpm).

Differences in the number of records with TWA were evaluated with the Fisher's exact test; differences in mean values of $V_{\max}$, $\mathcal{D}$, and HR_o were evaluated with the Mann–Whitney U-test. A p-value <0.05 was considered significant.

TABLE I
RESULTS OF TWA ANALYSIS IN STRESS TEST DATA, CALCULATED CONSIDERING ALL EPISODES REGARDLESS OF WHEN THEY ARE DETECTED

			MULTILEAD		SINGLE-LEAD	
			volunteer	ischemic	volunteer	ischemic
Detection		*# records*	66	70	66	70
		# records with TWA	26	27	19	20
		% records with TWA	39.39	38.57	28.79	28.57
TWA characteristics	all episodes detected by each scheme	V_{max} (μV)	85±114‡	95±128	133±133‡	135±146
		$\mathcal{D}$ (*s*)	26±26	48±59	29±24	51±39
		HR_o (*bpm*)	124±30†	106±20†	121±30†	105±20†
		# episodes	38	33	26	22
	episodes detected by one scheme and not by the other	V_{max} (μV)	21±15†‡	37±22†	52±35‡	66±35
		$\mathcal{D}$ (*s*)	7±7	30±71	17±16	18±21
		HR_o (*bpm*)	127±27†	107±19†	112±7	105±18
		# episodes	17	18	5	7

$P_{FA} = 0.01$ for the two schemes. Data expressed as (mean ± one standard deviation). †indicates a significant difference between volunteer and ischemic group; ‡indicates a significant difference between multilead and single-lead schems.

TABLE II
RESULTS OF NUMBER OF RECORDS WITH TWA IN STRESS TEST DATA, CALCULATED CONSIDERING EPISODES DETECTED BEFORE HEART RATE REACHES 110 BPM (FIRST ROW) AND 100 BPM (SECOND ROW)

		MULTILEAD		SINGLE-LEAD	
		volunteer	ischemic	volunteer	ischemic
Detections with HR_o < 110 bpm	*# records*	66	70	66	70
	# records with TWA	6†	14†	6	12
	% records with TWA	9.09†	20.00†	9.09	17.14
Detections with HR_o < 100 bpm	*# records*	66	70	66	70
	# records with TWA	6†	14†	5	10
	% records with TWA	9.09†	20.00†	7.58	14.29

$P_{FA} = 0.01$ for the two schemes. †indicates a significant defference in the number of records with TWA in volunteer and ischemic groups.

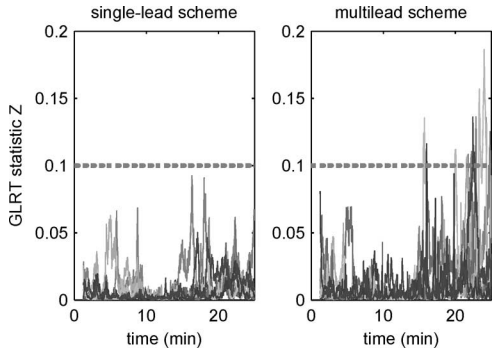

Fig. 9. Detection statistic Z of LLR method computed with a 128-beat window in signal Sig1. (Left) Z obtained with the single-lead scheme in leads V1–V6, I, and II after the preprocessing stage. (Right) Z obtained with the multilead scheme in transformed leads T1–T8 after PCA transformation. Threshold $\gamma = 0.1$ is shown as dashed line.

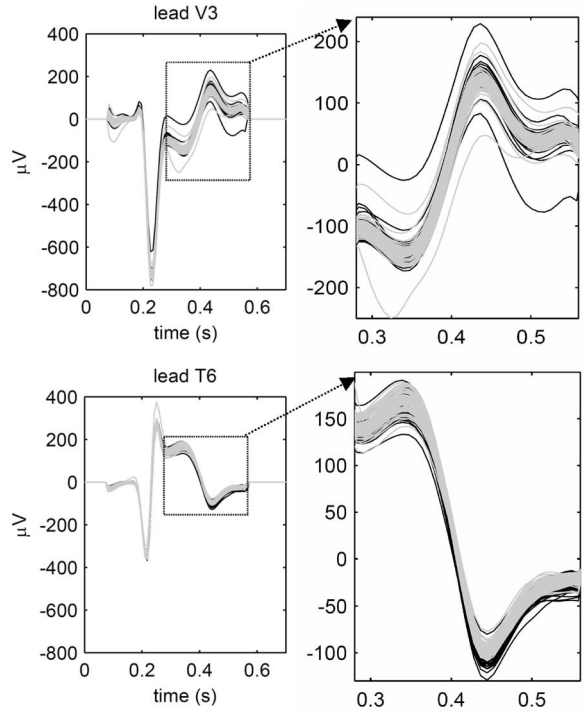

Fig. 10. Superposition of odd (black) and even (gray) beats of a 128-beat analysis window centered on instant $t_{\max} = 24$ min in signal Sig1. (Top) Beats of lead V3 (left), which is the lead where the maximum Z appears with the single-lead scheme, and a closer view of the ST-T complexes (right). (Bottom) Same views for lead $T6$, where the maximum Z appears with the multilead scheme. In this case, ST-T complex morphology is consistently different in odd and even beats, making TWA visible to the naked eye.

As an illustrative example, Figs. 9–11 show how the schemes work with a signal belonging to the ischemic group (Sig1). Fig. 9 shows the detection statistic Z obtained with the two schemes. The maximum value of Z for the multilead scheme appears at instant $t_{\max} = 24$ min. At that time, the maximum Z with the single-lead scheme is obtained in lead V3 and with the multilead scheme in T6. Fig. 10 shows the superposition of even and odd beats in these leads. Fig. 11 shows the estimated TWA waveform in Sig1 at $t_{\max}$. A detection threshold $\gamma = 0.1$ was used with the multilead scheme, and therefore, lead T6 was the only one considered in the reconstruction stage.

V. DISCUSSION

According to simulation results, the high detection performance of the multilead scheme is similar for gs, lp, and ma noises (Fig. 4). It is worse when facing em noise, because the em bandwidth mostly overlaps the band of the TWA. Even in this case, the multilead scheme performs better than the single-lead scheme. Note that in Fig. 4, the single-lead scheme is not capable of detecting anything due to the low SNR level.

As shown in Fig. 5, the multilead scheme surpasses widely the performance of the single-lead scheme. The multilead scheme detects TWA with an SNR from 27 to 30 dB lower than the single-lead scheme for a fixed $P_{\rm D}$. The multilead scheme

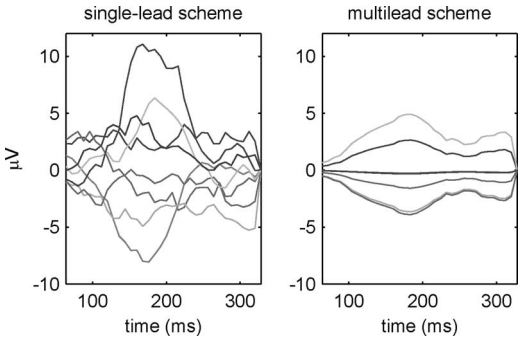

Fig. 11. TWA waveform estimated in Sig1 at $t_{\max} = 24$ min (left) with the single-lead scheme and (right) the multilead scheme with $\gamma = 0.1$ (right).

performs better, especially at low SNR levels, because it separates TWA from most of the noise. For instance, at SNR $= -20$ dB, noise is mainly concentrated in leads T1–T3, so TWA becomes detectable in leads T5–T7 [Fig. 2(c)].

In the example signal Sig1, the values of the detection statistic Z are higher with the multilead scheme than with the single-lead scheme (Fig. 9). Since the detector is CFAR, a higher $P_{\rm D}$ can be obtained for a fixed threshold or a lower number of false detections for a given $P_{\rm D}$. The main effect of PCA in this case is concentrating the noise in the first transformed leads, making TWA detectable in lead T6 (note that TWA is clearly visible in T6, but not in V3). With real signals, PCA will work differently depending on the spatial autocorrelation of noise and TWA, and the cross-correlation between them. It may concentrate mainly the noise, the TWA, or both. In the worst situation, when the correlations of noise and TWA are similar, they will not be separated at all. In that case, the multilead scheme will not improve the analysis, but it will not make the result worse either.

Since the improvement obtained with the multilead scheme is mainly due to the effect of PCA, similar detection gains can be expected when combining the multilead scheme with other TWA techniques. For example, in simulated data with ma noise, applying the multilead scheme to the SM yields an improvement of 30 dB over the single-lead approach, which is similar to the improvement obtained by applying the multilead scheme to the LLR method (28 dB) (Fig. 8).

The multilead scheme also improves the estimation accuracy, although not so remarkably as the probability of detection. For high SNR levels, the bias of the multilead estimation is higher than the bias of the single-lead estimation due to the truncation carried out in the reconstruction stage. As only a subset of transformed leads is used to reconstruct the signal, the reconstructed TWA lacks the content of the truncated leads, which may still contain a small alternant component. However, the lower variance of the multilead estimation compensates the bias, so the final relative error $\mathcal{R}_{e_l}$ is similar to the error of the single-lead estimation for high SNR levels (Fig. 7).

For low SNR levels, on the other hand, the relative bias of the single-lead estimation tends to 100% in all the leads, i.e., the estimation tends to zero. This is because as SNR decreases, the $P_{\rm D}$ of the single-lead scheme starts falling (see Fig. 5), so the estimated value is zero in more and more realizations. In this case, the behavior of the multilead scheme is better because the relative bias of the multilead estimation varies differently for each lead, and for some of them, it is still lower than 50% at very low SNR levels. For example, $\mathcal{R}_{b_l} < 50\%$ in V1, V4, V5, and V6 until SNR $= -45$ dB for ma noise (Fig. 7). When SNR < -25 dB, $\mathcal{R}_{e_l} > 100\%$ in the eight leads for the single-lead estimation, whereas with the multilead estimation, such degradation does not appear until SNR < -50 dB.

In the example signal Sig1 (Fig. 11), the estimation obtained with the multilead scheme may have bias, but is still useful to study the TWA distribution along the ST-T complex. With the single-lead scheme, this episode would not be detected with $\gamma = 0.1$ (Fig. 9), and even with a low enough threshold, the single-lead estimation would be much noisier, reducing its clinical value.

In simulation, the multilead scheme yields an improvement of the probability of detection and a more accurate estimation; results obtained in the real dataset prove that these benefits can also be obtained with real signals. As shown in Table I, the multilead scheme detects more episodes than the single-lead scheme in both groups (26 versus 19 in volunteers, 27 versus 20 in ischemics). Since the $P_{\rm FA}$ of both schemes is the same, this means that the detection power of this scheme is higher than the detection power of the single-lead scheme.

When considering the episodes detected only by the multilead scheme, episodes from volunteers have significantly lower amplitude than episodes from ischemics (21 ± 15 versus 37 ± 22 μV) and they appear at a higher HR$_o$ (127 ± 27 versus 107 ± 19 bpm). These differences are not significant with the single-lead scheme. In volunteers, episodes detected only by the multilead scheme have a significantly lower amplitude than episodes detected only by the single-lead scheme (21 ± 15 versus 52 ± 35 μV), and a higher HR$_o$ (127 ± 27 versus 112 ± 7 bpm); this suggests that the multilead scheme detects low-amplitude episodes near the peak effort that the single-lead scheme cannot detect.

The percentage of records with TWA is similar in volunteer and ischemic groups, both with the multilead scheme (39% and 38%) and with the single-lead scheme (28% in both groups). This can be due to the fact that volunteers reach a higher peak heart rate during the test. To distinguish between groups according to the risk of SCD, it is necessary to analyze only the results obtained before the heart rate reaches a cutoff point. When the multilead scheme is applied, the percentage of records with TWA is significantly higher in the ischemic group for any cutoff point between 100 and 110 bpm, whereas this difference is not significant with the single-lead scheme (Table II). This suggests that the multilead scheme can improve the prognostic utility of the TWA test.

Several limitations of this study must be acknowledged. Regarding simulated data, physiological features of ECG repolarization such as shape variation due to heart rate variability or amplitude modulation due to the respiration have not been included in the simulation setup. Moreover, the noise spatial correlation and the TWA waveform used in the simulation are two particular cases, but strong differences can be found in the lead distribution of noise and TWA in real ECG signals [8].

Regarding stress test data, the use of Bruce protocol may reduce the utility of the TWA test, because the increase in heart rate from 100 to 110 bpm occurs too rapidly, and may not permit enough time for TWA to develop. The use of Bruce protocol does not pose a problem in this paper, because the study is aimed to compare detection and estimation of the two schemes, but it should be avoided in future clinical studies regarding TWA stress testing. Finally, results suggest that the multilead scheme might improve the prognostic utility of the test, but the follow-up information of the study population is not available, and therefore, the determination of a cutoff heart rate to predict cardiovascular events, or the evaluation of the prognostic value of detected episodes, is out of the scope of this paper.

VI. Conclusion

A novel multilead scheme to detect and estimate TWA in the ECG was proposed. The proposed scheme was validated in terms of detection performance and estimation accuracy, and it was compared to a single-lead scheme. Simulation results showed the advantages of using PCA to exploit the spatial redundancy of multilead ECG signals. Combination of the multilead scheme with the LLR method showed the best improvement in the ability to detect low-amplitude TWA, outperforming the single-lead approach of the LLR method, and both single and multilead approaches of the SM.

Results in real stress test ECG records confirmed the higher detection power of the multilead scheme and showed that the detections obtained with this scheme are significantly different in healthy volunteers and ischemic patients, whereas they are not with the single-lead scheme. The positive results of this methodological evaluation suggest that the proposed multilead approach can be highly useful in future clinical studies to increase the prognostic value of TWA tests.

References

[1] D. S. Rosenbaum, L. E. Jackson, J. M. Smith, H. Garan, J. N. Ruskin, and R. J. Cohen, "Electrical alternans and vulnerability to ventricular arrhythmias," *N. Engl. J. Med.*, vol. 330, no. 4, pp. 235–241, 1994.

[2] S. M. Narayan, "T-wave alternans and the susceptibility to ventricular arrhythmias," *J. Amer. Coll. Cardiol.*, vol. 47, no. 2, pp. 269–281, 2006.

[3] J. P. Martínez and S. Olmos, "Methodological principles of T wave alternans analysis: A unified framework," *IEEE Trans. Biomed. Eng.*, vol. 52, no. 4, pp. 599–613, Apr. 2005.

[4] J. M. Smith, E. A. Clancy, C. R. Valeri, J. N. Ruskin, and R. J. Cohen, "Electrical alternans and cardiac electrical instability," *Circulation*, vol. 77, no. 1, pp. 110–121, 1988.

[5] B. D. Nearing and R. L. Verrier, "Modified moving average analysis of T-wave alternans to predict ventricular fibrillation with great accuracy," *J. Appl. Physiol.*, vol. 92, no. 2, pp. 541–549, 2002.

[6] B. D. Nearing, A. H. Huang, and R. L. Verrier, "Dynamic tracking of cardiac vulnerability by complex demodulation of the T wave," *Science*, vol. 252, no. 5004, pp. 437–440, 1991.

[7] J. P. Martínez and S. Olmos, "Detection of T wave alternans in nonstationary noise: A GLRT approach," in *Proc. Comput. Cardiol. 2003*. Los Alamitos, CA: IEEE Comput. Soc. Press, pp. 161–164.

[8] J. P. Martínez, S. Olmos, G. Wagner, and P. Laguna, "Characterization of repolarization alternans during ischemia: Time-course and spatial analysis," *IEEE Trans. Biomed. Eng.*, vol. 53, no. 4, pp. 701–711, Apr. 2006.

[9] S. M. Narayan and J. M. Smith, "Differing rate dependence and temporal distribution of repolarization alternans in patients with and without ventricular tachycardia," *J. Cardiovasc. Electrophysiol.*, vol. 10, pp. 61–71, 1999.

[10] F. Castells, P. Laguna, L. Sörnmo, A. Bollmann, and J. M. Roig, "Principal component analysis in ecg signal processing," *EURASIP J. Appl. Signal Process.*, vol. 2007, no. 1, pp. 98–98, 2007.

[11] S. O. Gasso, J. G. Moros, J. Jané, and P. L. Lasaosa, "ECG signal compression and noise filtering with truncated orthogonal expansion," *Signal Procesing*, vol. 79, no. 1, pp. 97–115, 1999.

[12] B. Acar and H. Köymen, "SVD-based on-line exercise ECG signal orthogonalization," *IEEE Trans. Biomed. Eng.*, vol. 46, no. 3, pp. 311–312, Mar. 1999.

[13] J. Paul, M. Reddy, and V. Kumar, "A transform domain SVD filter for suppression of muscle noise artefacts in exercise ECGs," *IEEE Trans. Biomed. Eng.*, vol. 47, no. 5, pp. 654–663, May 2000.

[14] J.-J. Wei, C.-J. Chang, N.-K. Chou, and G.-J. Jan, "ECG data compression using truncated singular value decomposition," *IEEE Trans. Inf. Technol. Biomed.*, vol. 5, no. 4, pp. 290–299, Dec. 2001.

[15] J. García, G. Wagner, L. Sörnmo, P. Lander, and P. Laguna, "Identification of the occluded artery in patients with myocardial ischemia induced by prolonged percutaneous transluminal coronary angioplasty using traditional vs transformed ECG-based indexes," *Comput. Biomed. Res.*, vol. 32, no. 5, pp. 470–482, 1999.

[16] J. García, M. Ansträm, J. Mendive, P. Laguna, and L. Sörnmo, "ECG-based detection of body position changes in ischemia monitoring," *IEEE Trans. Biomed. Eng.*, vol. 50, no. 6, pp. 677–685, Jun. 2003.

[17] E. Pueyo, J. P. Martínez, and P. Laguna, "Cardiac repolarisation analysis using the surface ECG," *Phil. Trans. R. Soc. A*, vol. 367, pp. 213–233, 2009.

[18] P. Okin, R. Devereux, R. Fabsitz, E. Lee, J. Galloway, and B. Howard, "Principal component analysis of the T wave and prediction of cardiovascular mortality in american indians: The strong heart study," *Circulation*, vol. 105, pp. 714–719, 2002.

[19] G. Acar, G. Yi, K. Hnatkova, and M. Malik, "Spatial, temporal and wavefront direction characteristics of 12-lead T wave morphology," *Med. Biol. Eng. Comput.*, vol. 37, pp. 574–584, 1999.

[20] L. Faes, G. Nollo, M. Kirchner, E. Olivetti, F. Gaita, and R. Antolini, "Principal component analysis and cluster analysis for measuring the local organization of human atrial fibrillation," *Med. Biol. Eng. Comput.*, vol. 39, pp. 656–663, 2001.

[21] F. Castells, J. J. Rieta, J. Millet, and V. Zarzoso, "Spatiotemporal blind source separation approach to atrial activity estimation in atrial tachyarrhythmias," *IEEE Trans. Biomed. Eng.*, vol. 52, no. 2, pp. 258–267, Feb. 2005.

[22] P. Kanjilal, S. Palit, and Saha, "Fetal ECG extraction from single-channel maternal ECG using singular value decomposition," *IEEE Trans. Biomed. Eng.*, vol. 44, no. 1, pp. 51–59, Jan. 1997.

[23] J. P. Martínez, R. Almeida, S. Olmos, A. P. Rocha, and P. Laguna, "A wavelet-based ECG delineator: Evaluation on standard databases," *IEEE Trans. Biomed. Eng.*, vol. 51, no. 4, pp. 570–581, Apr. 2004.

[24] G. B. Moody, W. Muldrow, and R. G. Mark, "A noise stress test for arrhythmia detectors," in *Proc. Comput. Cardiol. 1984*. Los Alamitos, CA: IEEE Comput. Soc. Press, vol. 11, pp. 381–384.

[25] R. Bousseljot, D. Kreiseler, and A. Schnabel, "Nutzung der EKG-Signaldatenbank CARDIODAT der PTB über das internet," *Biomed. Tech.*, vol. 40, pp. 317–318, 1995.

[26] G. H. Golub and C. F. Van Loan, *Matrix Computations*, 2nd ed. Baltimore, MD: The Johns Hopkins Univ. Press, 1989.

[27] R. Bailón, J. Mateo, S. Olmos, P. Serrano, J. García, A. del Río, I. J. Ferreira, and P. Laguna, "Coronary artery disease diagnosis based on exercise electrocardiogram indexes from repolarisation, depolarisation and heart rate variability," *Med. Biol. Eng. Comput.*, vol. 41, no. 5, pp. 561–571, 2003.

Violeta Monasterio received the M.Sc. degree in telecommunication engineering in 2005 from the University of Zaragoza, Zaragoza, Spain, where she is currently working toward the Ph.D. degree in biomedical engineering.

She is with the Centro de Investigación Biomédica en Red en Bioingeniería, Biomateriales y Nanomedicina (CIBER-BBN), University of Zaragoza. Her current research interests include the field of biomedical signal processing and the study of the electrocardiographic signal.

Pablo Laguna (M'92–SM'06) was born in Huesca, Spain, in 1962. He received the M.S. degree in physics and the Ph.D. degree from the Science Faculty, University of Zaragoza, Zaragoza, Spain, in 1985 and 1990, respectively.

He was at the Biomedical Engineering Division, Institute of Cybernetics (U.P.C.-C.S.I.C.). He is currently a Full Professor of signal processing and communications in the Department of Electrical Engineering, Engineering School, University of Zaragoza, where he was an Associated Professor from 1992 to 2005 and is currently a Researcher at Aragón Institute for Engineering Research (I3A). From 1987 to 1992, he was an Assistant Professor of automatic control in the Department of Control Engineering, Politecnic University of Catalonia (U.P.C.), Spain, and a Researcher at the Biomedical Engineering Division, Institute of Cybernetics (U.P.C.-C.S.I.C.). His current research interests include signal processing, in particular applied to biomedical applications. He is the author of *Bioelectrical Signal Processing in Cardiac and Neurological Applications* (Elsevier, 2005).

Juan Pablo Martínez was born in Zaragoza, Aragón, Spain, in 1976. He received the M.S. degree in telecommunication engineering and the Ph.D. degree in biomedical engineering from the University of Zaragoza (UZ), Zaragoza, in 1999 and 2005, respectively.

Since 2000, he has been an Assistant Professor in the Department of Electronic Engineering and Communications, UZ, where he has been an Associate Professor since 2007, is currently a Researcher at the Aragón Institute for Engineering Research (I3A), and is also with the Centro de Investigación Biomédica en Red en Bioingeniería, Biomateriales y Nanomedicina (CIBER-BBN). His current research interests include biomedical signal processing, with main interest in signals of cardiovascular origin.